Metastable Structures and Recombination Pathways for Atomic Hydrogen on the Graphite (0001) Surface

L. Hornekær,[1,*] Ž. Šljivančanin,[2] W. Xu,[1] R. Otero,[1,†] E. Rauls,[1] I. Stensgaard,[1] E. Lægsgaard,[1] B. Hammer,[1] and F. Besenbacher[1]

[1]*Interdisciplinary Nanoscience Center (iNANO) and Department of Physics and Astronomy, University of Aarhus, Ny Munkegade bygning 1520, 8000 Aarhus C, Denmark*

[2]*Ecole Polytechnique Fédérale de Lausanne (EPFL), ITP and IRRMA, CH-1015 Lausanne, Switzerland*

(Received 20 October 2005; published 20 April 2006)

We present scanning tunneling microscopy results which reveal the existence of two distinct hydrogen dimer states on graphite basal planes. Density functional theory calculations allow us to identify the atomic structure of these states and to determine their recombination and desorption pathways. Direct recombination is only possible from one of the two dimer states. This results in increased stability of one dimer species and explains the puzzling double peak structure observed in temperature programmed desorption spectra for hydrogen on graphite.

DOI: 10.1103/PhysRevLett.96.156104 PACS numbers: 68.43.−h, 68.37.Ef, 82.65.+r

The interaction between molecular and atomic hydrogen and graphite surfaces has attracted considerable interest in recent years. The possibility of using carbon nanostructures as a storage medium for hydrogen has been extensively investigated [1], and it has been suggested that hydrogen atoms stored in the chemisorbed state of graphite might be an energy source for future space applications due to the high energy release in molecular hydrogen formation from atomic recombination on this surface [2]. In the area of interstellar chemistry, hydrogen on graphite is considered to be a key model system. In spite of continuous destruction by UV radiation and cosmic rays, H_2 is the most abundant molecule in the interstellar medium (ISM). However, no efficient gas-phase route exists for H_2 formation at the low H-atom densities of the ISM. Thus, efficient formation of H_2 in interstellar dust and molecular clouds is believed to proceed via atomic recombination of hydrogen atoms adsorbed on interstellar dust grain surfaces. Recent experiments have shown that such processes are indeed possible under conditions resembling those found in dense and cold (10–20 K) diffuse interstellar clouds [3–5]. However, the mechanisms suggested by these experiments are all based on recombination of physisorbed atomic hydrogen and are efficient only in a small temperature interval [3]. Hence, they cannot explain efficient formation under conditions found in warmer environments such as photo dissociation regions (PDRs), where more tightly bound, chemisorbed, states of adsorbed hydrogen atoms have to be invoked [6]. Since carbonaceous grains are believed to be abundant in the ISM, particular attention has been focused on atomic recombination of hydrogen adsorbed in chemisorbed states on graphite surfaces [6].

The chemisorbed state of atomic hydrogen on graphite was initially observed using ultraviolet photon spectroscopy [7], and its characteristics were predicted by density functional theory calculations. The calculations show that hydrogen binds with a binding energy of ~0.7 eV at an on-top site, causing a reconstruction of the graphite surface in which the C atom below the H atom puckers out of the surface by 0.35 Å [8,9]. Because of this puckering there is a barrier to enter into the chemisorption state of about 0.2 eV [8,9]. Atomic recombination to molecular hydrogen from chemisorbed atomic hydrogen on graphite has been observed in temperature programed desorption (TPD) measurements [10] and via Eley-Rideal processes [11]. The TPD spectra are 1st order suggesting that the H atoms might be paired on the surface prior to desorption or that the rate limiting step in the recombination process involves only one H atom. Also, the spectra exhibit a double peak structure indicative of multiple adsorption sites and desorption pathways. In spite of increased theoretical activity aimed at determining the mobility of hydrogen atoms [10,12] and the binding energy of hydrogen dimer states [12,13] on graphite, the recombination pathways for hydrogen atom adsorbates on graphite surfaces are still undetermined.

In this Letter, we report on STM experiments combined with density functional theory (DFT) calculations, which clarify both the structures and kinetic recombination pathways of different hydrogen dimer states on highly oriented pyrolithic graphite (HOPG). At low coverage, recombination is seen to take place out of only one hydrogen adsorbate dimer state, in which hydrogen atoms are adsorbed on carbon atoms on opposite sides of the carbon hexagon. All other states, including the nearest neighbor dimer state, are observed to recombine via diffusion over this state. These results explain the structure observed in TPD spectra of molecular hydrogen desorption from graphite.

All experiments were performed using the home built Aarhus STM [14] under ultrahigh vacuum (UHV) at a base pressure below 3×10^{-10} Torr. HOPG samples were cleaved in air immediately prior to being inserted into the UHV chamber. In vacuum the samples were annealed

to 1300 K by electron bombardment of the sample backside to desorb any hydrogen or oxygen bound at the surface and at step edges or defects. Atomic hydrogen dosing was performed using a hot (2200 K) hydrogen atom beam source (HABS 40 from MBE Komponenten). The adsorption of hydrogen on the HOPG surface was confirmed by TPD experiments into a differentially pumped quadrupole mass spectrometer (QMS), equipped with a Fuelner cap cone with a 3 mm opening, which can be moved to within 1 mm of the sample surface. In the majority of the experiments, deuterium atoms were used to obtain a better signal-to-background ratio in the TPD experiments. All temperature measurements were performed by a type K thermocouple mounted on the backside of the HOPG sample.

The density functional theory calculations were performed with the computer code DACAPO [15], using ultrasoft pseudopotentials [16,17] and plane waves (wave function/density cutoff: 25/140 Ry). The C(0001) surface was modeled by a graphene sheet containing 50 atoms in the periodically repeated supercell. Test calculations with two graphene layers showed negligible change in the H binding energy. The electronic exchange-correlation effects were described by the revised Perdew-Burke-Ernzerhof (RPBE) functional [15]. Simulated STM images are topographs of constant local density of states, $\rho(x, y, z, \varepsilon) = \rho_0$ [18]. The energy, ε, was chosen as the Fermi level off set by the experimental tunneling voltage, V_t, and ρ_0 was chosen so that the magnitude of the experimental and simulated corrugation became comparable. Diffusion barriers were calculated using the nudged elastic band method [19].

Figure 1(a) shows an STM image of the graphite surface after a 1 min dose of D atoms at 2200 K onto a room temperature HOPG sample. A number of bright protrusions are observed in the image (the coverage is approximately 1%), which we identify as clusters of chemisorbed deuterium atoms, as they only appear after D dosing. As discussed below, their presence correlates with the D_2 desorption peaks observed in the TPD spectra. The deuterium atoms are not observed to diffuse at room temperature. In between the bright protrusions, the graphite lattice is observed. Associated to each bright D atom correlated protrusion, we find a wavelike electronic perturbation of the graphite lattice, which vanishes for distances larger than about 35 Å. This is in good agreement with previous results for H implanted on HOPG by hydrogen plasma treatment [20]. In accordance with earlier observations, no well-ordered superstructure of the adsorbed deuterium atoms is observed. Two different characteristic structures, labeled dimer A and dimer B, are observed to be dominant, with the dimer B structure as the most numerous. Figs. 1(b) and 1(c) show closeups of these two structures. Dimer A are slim elongated spheroids, while dimer B structures are more rectangular in shape. The long axis of both dimer A and dimer B structures is oriented along directions offset 30° with respect to the $\langle 2\bar{1}\,\bar{1}\,0\rangle$ directions. This results in three possible orientations separated 120° with respect to each other. A few larger, composite structures are also observed.

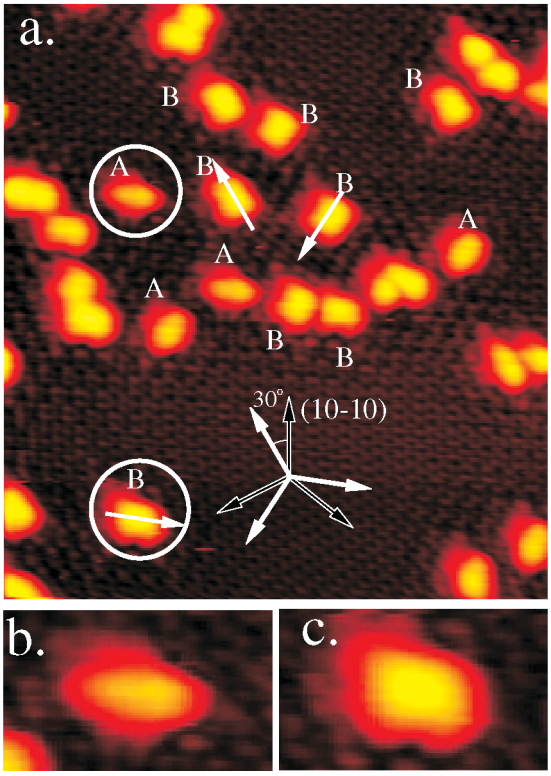

FIG. 1 (color). (a) STM image (103 × 114 Å^2) of dimer structures of hydrogen atoms on the graphite surface after a 1 min deposition at room temperature. Imaging parameters: V_t = 884 mV, I_t = 160 pA. Examples of dimer type A and B are marked. Black arrows indicate the $\langle 2\bar{1}\,\bar{1}\,0\rangle$ directions and white arrows indicate the orientation of the dimers 30° off. (b) Close up of dimer A structure in top white circle in image (a). (c) Close up of dimer B structure in lower white circle in image (a).

Figure 2(a) shows a D_2 TPD spectrum from the HOPG surface after a 2 min D atom dose. The spectrum shows the double peak structure discussed in the introduction. In order to investigate if the peaks correspond to different hydrogen adsorbate structures, we performed a thermal anneal to a temperature between the two peaks. The arrow indicates the maximum temperature (525 K) of the thermal anneal performed before recording the STM image shown in Fig. 2(b). After the 525 K anneal, the sample is cooled to room temperature before being placed in the STM. We find a significant decrease in the total coverage on the annealed sample, and now only dimer A structures are observed. Repeated experiments showed that annealing to temperatures of 500–600 K starting from a low coverage of D atoms leads to a surface where dimer A is the dominant structure. Hence, the experiment indicates that dimer A structures are stable against thermal annealing to 525 K, whereas dimer B structures are not. Since no D atoms are visible on the surface after anneals to 600 K, i.e., above the high temperature peak in the TPD spectrum, the interpretation is that dimer B structures contribute to the first peak

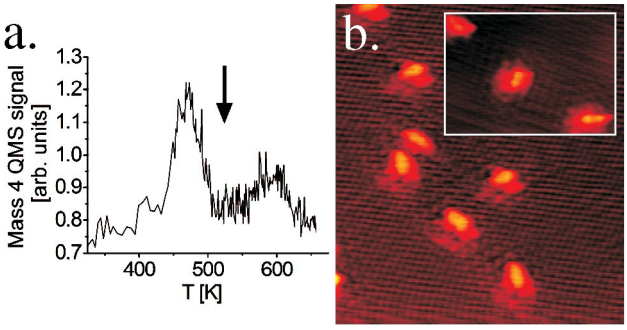

FIG. 2 (color). (a) A mass 4 amu, i.e., D_2, TPD spectrum from the HOPG surface after a 2 min D atom dose (ramp rate: 2 K/s below 450 K, 1 K/s above). The arrow indicates the maximum temperature of the thermal anneal performed before recording the STM image in (b) STM image (103×114 Å^2) of dimer structures of hydrogen atoms on the graphite surface after a 1 min deposition at room temperature and subsequent anneal to 525 K (ramp rate: 1 K/s, 30 s dwell at maximum temperature). Imaging parameters: $V_t = 884$ mV, $I_t = 190$ pA. The inset shows a higher resolution STM image of dimer structures of hydrogen atoms on the graphite surface after a 6 min deposition at room temperature and subsequent anneal to 550 K. Imaging parameters: $V_t = -884$ mV, $I_t = -210$ pA.

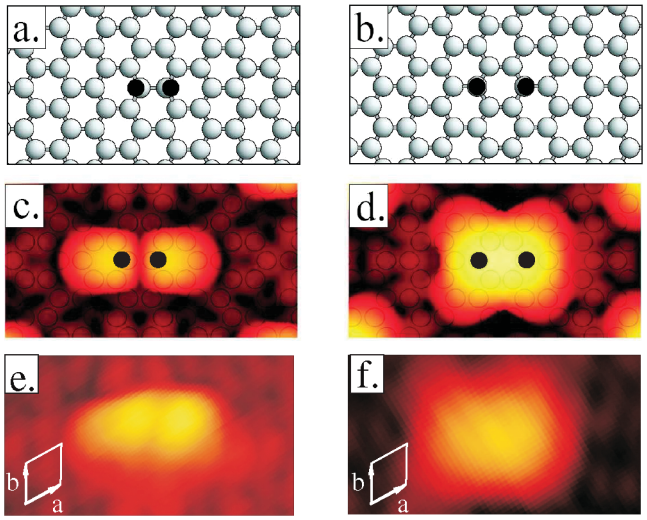

FIG. 3 (color). Calculated structure of the two most tightly bound dimer structures of hydrogen atoms on the graphite surface. (a) Dimer A structure of hydrogen atoms adsorbed on neighbor carbon atoms. (b) Dimer B structures of hydrogen adsorbed on carbon atoms at opposite sides of the graphite hexagon. (c) Simulated STM image of the dimer structure in (a). (d) Simulated STM image of the dimer structure in (b). Imaging parameters: $V_t = 0.9$ V, $\rho_0 = 1 \times 10^{-6}$ (eV)$^{-1}$ Å^{-3}. The position of the hydrogen atoms is marked by black dots. (e) Experimental dimer A structure. (f) Experimental dimer B structure. The carbon unit cell is marked in white.

in the desorption spectra while dimer A structures are associated with the second peak. Based on the Polanyi-Wigner equation for first order desorption and assuming a preexponential factor of 10^{13} s^{-1}, the two peaks at 490 K (445 K) and 580 K (560 K) observed in TPD spectra for deuterium (hydrogen) on graphite [10] correspond to desorption barriers of 1.38 eV (1.25 eV) and 1.64 eV (1.58 eV), respectively.

Density functional theory calculations of the lowest energy states of H dimers on a graphite surface show two states with an approximately identical binding energy of 2.51 eV with respect to the energy of the undisturbed carbon surface and 2 H atoms at infinite separation. Referring to two isolated adsorbed H atoms the binding energy is 1.18 eV. The two states are shown in Figs. 3(a) and 3(b). The two hydrogen atoms are adsorbed either on two neighbor carbon atoms or on carbon atoms at opposite sides of a carbon hexagon. Based on the structure and stability findings given below we assign the state shown in Fig. 3(a) to the experimentally observed dimer A and the state in Fig. 3(b) to the experimental dimer B state. The calculated binding energy of the dimer A state is in good agreement with earlier calculations [12,13]. However, the binding energy of the dimer B state differs from that reported in Miura *et al.* [13]. This difference can be ascribed to the fact that a smaller carbon unit cell was used in the previous calculations [13]. Figs. 3(c) and 3(d) show simulated STM images of the two dimer structures. In both cases the dimers and the long axis of the dimer structures in the simulated images are oriented at 30° with respect to the $\langle 2\bar{1}\,\bar{1}\,0\rangle$ directions, like the experimentally observed dimer structures. The dimer structure shown in Fig. 3(c) is an elongated spheroid with a thin dark central line structure along the minor axis. The simulated image is very reminiscent of the dimer A structure in the experimental images. However, due to tip smoothing effects the thin dark central line is only imaged in STM under very favorable imaging conditions as in the inset in Fig. 2(b) and in Fig. 3(e). The dimer structure in Fig. 3(d) on the other hand is more rectangular in shape and resembles the dimer B structures observed in the STM images.

Since each dimer corresponds to a different peak in the TPD spectra, dimer A must be more stable than dimer B. Clearly, this difference in stability cannot be explained by binding energy considerations. Instead, the detailed kinetics of the desorption processes has to be considered and the recombination pathways for each of the two dimer states identified. Figure 4 shows the calculated binding energies, diffusion barriers and recombination barriers for 2 H atoms on the graphite surface. Based on the calculations, it becomes clear that recombination will take place out of the dimer B state with a barrier of 1.4 eV, in reasonable agreement with the barrier derived from the first peak in the TPD spectra. Direct recombination from the dimer A state into molecular hydrogen is prevented by a rather large energy barrier, similar to the energy cost to desorb both H atoms separately. A facile pathway for recombination of hydrogen atoms in the dimer A state can, however, be found, corresponding to diffusion over state I into state B and then direct recombination from B. The rate limiting step in this process is diffusion from state A to state I. The diffusion barrier is

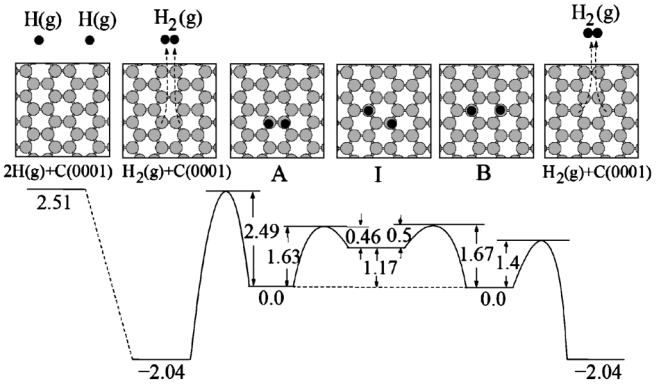

FIG. 4. Energy barriers for atomic hydrogen diffusion and recombination from dimer A and B states on the graphite surface. The barrier to desorption of a single H atom out of structures A, I, and B are 2.08, 0.92, and 1.92 eV, respectively, and is hence energetically unfavorable in all three cases.

1.6 eV, which is in excellent agreement with the barrier to desorption derived for the 2nd peak in the TPD spectra. Hence, direct recombination of dimers in a dimer B structure contribute to the low temperature peak in TPD, while diffusion mediated recombination from the dimer A state over the dimer B state contributes to the high temperature peak.

It has previously been suggested that recombination might occur via a physisorption state of H on graphite [21]. This suggestion was based on TPD experiments performed after H/D atom deposition at 150 K. Since the TPD spectra look identical for H/D atom deposition at 150 and 300 K [2] we expect recombination to proceed via the same pathway in the experiments reported on in [10,21] and the experiments reported on here. A weak physisorption state of H on graphite has been observed experimentally in scattering experiments [22] and theoretically in DFT calculations [8,9]. The binding energy of this state is of the order of a few tens of meV. Hence, recombination of two chemisorbed H atoms via this state would require that a hydrogen atom desorbs from the strongly bound chemisorbed state involving severe surface reconstruction and is readsorbed in a very shallow (10–40 meV) physisorption well. Such a process does not seem likely. The self-consistent model presented here offers an alternative explanation for recombination of atomic hydrogen on graphite surfaces that does not invoke recombination via a weakly bound physisorbed state.

In conclusion, based on STM experiments and DFT calculations we have identified the recombination mechanisms of H atoms on the graphite surface and shown that direct recombination takes place out of only one of the two observed dimer states. The presented results explain the structure observed in TPD spectra of molecular hydrogen desorption from graphite. Furthermore, the determined recombination mechanism and diffusion and recombination barriers provide direct input to models of interstellar hydrogen formation on graphitic interstellar dust grain surfaces.

We wish to thank Maya Schöck for useful discussions and advice. L. H. acknowledges support from the Danish National Research Council. R. O. acknowledges support from the EU through an individual Marie Curie Fellowship and the program NAMASOS. Calculations were performed at the central computational facilities of the Ecole Polytechnique Fédérale de Lausanne, the Swiss Center for Scientific Computing, and the Danish Center for Scientific Computing.

*Electronic address: liv@phys.au.dk
†Present address: Departmento de Física de la Materia Condensada, Universidad Autónoma de Madrid, 28049 Madrid, Spain.

[1] L. Schlapbach and A. Züttel, Nature (London) **414**, 353 (2001).
[2] S. Baouche, G. Gamborg, L. Hornekaer, V. V. Petrunin, A. C. Luntz, and A. Baurichter (to be published).
[3] N. Katz, I. Furman, O. Biham, V. Pironello, and G. Vidali, Astrophys. J. **522**, 305 (1999).
[4] G. Manico, G. Raguni, V. Pironello, J. Roser, and G. Vidali, Astrophys. J. **548**, L253 (2001).
[5] L. Hornekær, A. Baurichter, V. Petrunin, D. Field, and A. C. Luntz, Science **302**, 1943 (2003).
[6] S. Cazaux and A. Tielens, Astrophys. J. **604**, 222 (2004).
[7] D. Neumann, G. Meister, U. Kurpick, A. Goldmann, J. Roth, and V. Dose, Appl. Phys. A **55**, 489 (1992).
[8] L. Jeloaica and V. Sidis, Chem. Phys. Lett. **300**, 157 (1999).
[9] X. Sha and B. Jackson, Surf. Sci. **496**, 318 (2002).
[10] T. Zecho, A. Güttler, X. Sha, B. Jackson, and J. Küppers, J. Chem. Phys. **117**, 8486 (2002).
[11] T. Zecho, A. Güttler, X. Sha, D. Lemoine, B. Jackson, and J. Küppers, Chem. Phys. Lett. **366**, 188 (2002).
[12] Y. Ferro, F. Marinelli, and A. Allouche, Chem. Phys. Lett. **368**, 609 (2003).
[13] Y. Miura, H. Kasai, W. Dino, H. Nakanishi, and T. Sugimoto, J. Appl. Phys. **93**, 3395 (2003).
[14] E. Lægsgaard, F. Besenbacher, K. Mortensen, and I. Stensgaard, J. Microsc. **152**, 663 (1988).
[15] B. Hammer, L. B. Hansen, and J. K. Nørskov, Phys. Rev. B **59**, 7413 (1999).
[16] D. Vanderbilt, Phys. Rev. B **41**, R7892 (1990).
[17] K. Laasonen, A. Pasquarello, R. Car, C. Lee, and D. Vanderbilt, Phys. Rev. B **47**, 10 142 (1993).
[18] J. Tersoff and D. R. Hamann, Phys. Rev. B **31**, 805 (1985).
[19] H. Jónsson, G. Mills, and K. W. Jacobsen, in *Classical and Quantum Dynamics in Condensed Phase Simulations*, edited by B. J. Berne, G. Ciccoti, and D. F. Coker (World Scientific, Singapore, 1998).
[20] P. Ruffieux, O. Gröning, P. Schwaller, L. Schlapbach, and P. Gröning, Phys. Rev. Lett. **84**, 4910 (2000).
[21] T. Zecho, A. Güttler, and J. Küppers, Carbon **42**, 609 (2004).
[22] E. Ghio, L. Mattera, C. Salvo, F. Tommasini, and U. Valbusa, J. Chem. Phys. **73**, 556 (1980).